

9B.1 Assessment of Micro Rain Radar (MRR) observing network data and sensor density

Brian J. Etherton* and Jessica L. Proud
Renaissance Computing Institute (RENCI), University of North Carolina, Chapel Hill, NC

1. INTRODUCTION

In January of 2009, a significant ice storm impacted the state of Kentucky (Speath, et al, 2009, Grumm and LaCorte, 2009). Large areas of the state were impacted, with significant damage and loss of electricity resulting. A critical component in the formation of ice at the surface is the depth of the near-surface sub-freezing layer as well as the depth of the above-freezing layer above. Knowledge of the depth of both of these layers is helpful in determining surface precipitation type. Vertical profiles of the atmosphere are essential for determining the thicknesses of these layers. The number of vertical sounding profiles in the state of Kentucky is limited. There are no sounding sites in the state, and the nearby sounding sites (Nashville TN, Wilmington OH) only collect data every 12 hours.

Detection of the heights of the freezing layers during precipitation is possible with radar. This approach is limited by the horizontal resolution of the radar. Radar gates are hundreds of meters deep, and become deeper the further away from the radar. For example, 100km away from the radar site, the bottom-most radar gate is approximately 1km off the ground, and is 700-meters deep. Given the shallow nature of near-surface sub-freezing layers, the vertical resolution of standard WSR88D radar is not sufficient for resolving the freezing level.

An alternative is a micro rain radar (MRR). This vertically pointing radar can observe rain rate, liquid water content, fall velocity, and reflectivity – including the 'bright band'. The MRR has a vertical resolution of 150 meters, with the lowest gate at 150 meters above ground level. This sort of fidelity of vertical profile can resolve the near surface sub-freezing layer and overriding above-freezing layer – but only at one location. Given the relative costs of an MRR and a WSR88D (~\$20K vs ~\$2M), one could deploy a network of MRRs for the cost of one 88D. The question then is: what is the required network density required to accurately depict the altitude of the freezing levels.

Corresponding Author Address: 100 Europa Drive, Suite 540, Chapel Hill NC, 27517; email: etherton@renci.org

To assess the needed horizontal resolution of a MRR network, we conducted an observing system experiment. Using WRF to construct a nature run, we varied the density of hypothetical MRR sites.

2. WRF SIMULATION

In the spirit of an observing system experiment, the WRF model was run at high enough horizontal and vertical resolution to effectively simulate what an MRR would observe. WRF version 3.1 was run for a triple domain, shown in figure 1. The innermost domain had a resolution of 4/3km, 670x550 grid points, with 45 vertical levels. The physics options for this runs are as follows: for cloud microphysics, the Goddard 3ICE scheme (Tao *et al.* 2003; Lang *et al.* 2007) with snow, ice, and graupel, for shortwave and longwave radiation, the Community Atmosphere Model (CAM, Collins et al. 2004) schemes, for the boundary layer and surface layer, the quasi-normal scale elimination (QNSE, Sukoriansky et al. 2005) schemes, and for the soil layer, the NOAH land surface model (Ek et al., 2003). For this run we used This WRF model run was initialized using the NAM model, initialized at 0000 UTC on 27 January 2009. Our WRF simulation was 48 hours in length.

FIGURE 1

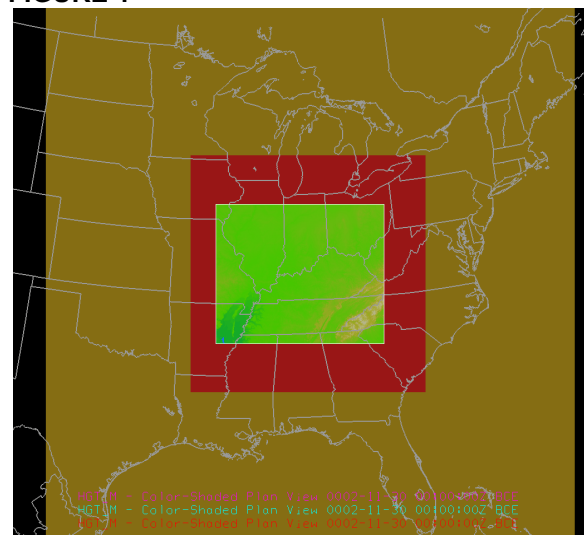


Figure 1. The domains for the WRF simulation. The resolution of the inner most domain (colors) is 4/3km, the middle domain (red) is 4km, and the outer domain (mustard) is 12km.

3. RESULTS

The first issue to address was whether or not there was a correlation between a parameter that the radar could observe and the height of the freezing level. Indeed, there was. Radar has a 'bright band' associated with the freezing level, and cross-sections indicated that radar reflectivity would peak at a freezing level. Figure 2 shows such a cross-section, with a peak in reflectivity near the freezing level. When looking from the ground up, the altitude of the 25dbz surface was at roughly the same altitude as the freezing level.

FIGURE 2

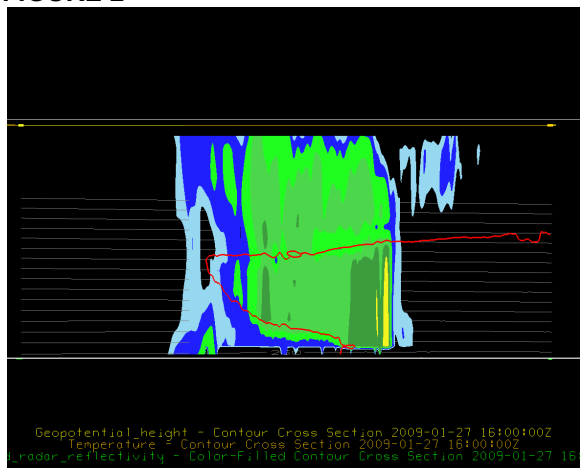


Figure 2. Cross section through 86W of simulated radar reflectivity (colors), and the height of the 0C isotherm (red line).

Given this correlation, we chose to compare the height of the first 25dbz layer encountered to the height of the first freezing level encountered if ascending from the surface. Figure 3 is such a comparison, for 1500 UTC on 27 January 2009. In northern and central Illinois, Indiana, and Ohio, the air is freezing from the surface through the atmosphere. In Tennessee, the air is above freezing through at least the bottom 2000 meters of the atmosphere. In between these areas the height of the freezing level transitions. There is a reasonable correlation between the height of the 25 dbz surface and the 0C surface, both transitioning from ground level in southern Illinois, Indiana, and Ohio to 2000m in Tennessee.

For the image shown in figure 3, these surfaces are calculated at all model gridpoints. For the 25 dbz surface, this is equivalent to having an MRR every 1.33km, which is not likely.

FIGURE 3

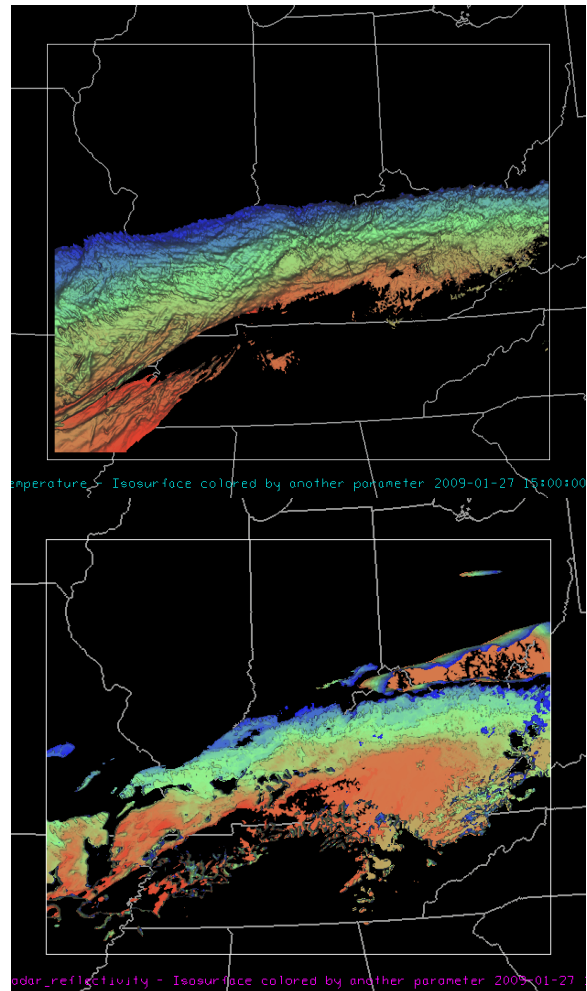


Figure 3. Height of the 0C isotherm (a) and height of the 25 dbz surface (b) in meters. Blue is 0 meters above ground level, red is 2000m above ground level. Model data from 1500 UTC on 27 January 2009.

We chose to think the number of MRR sites, selecting every 10th model grid point (13.3km resolution), every 20th model grid point (26.7km resolution), and every 50th model grid point (66.7km resolution). Figure 4 shows plots of the height of the 25dbz surface for those observing densities. The general pattern is the same in all three images, but the fidelity of the surface decreases as the observation density is lessened. Indeed, at a resolution of 66.7km, it is difficult to be confident in the heights observed.

The issue with the fidelity of the 25dbz surface is in the north-south direction, not the west-east direction. Indeed, even at the coarse 66.7km observing density, the transition zone is captured.

FIGURE 4

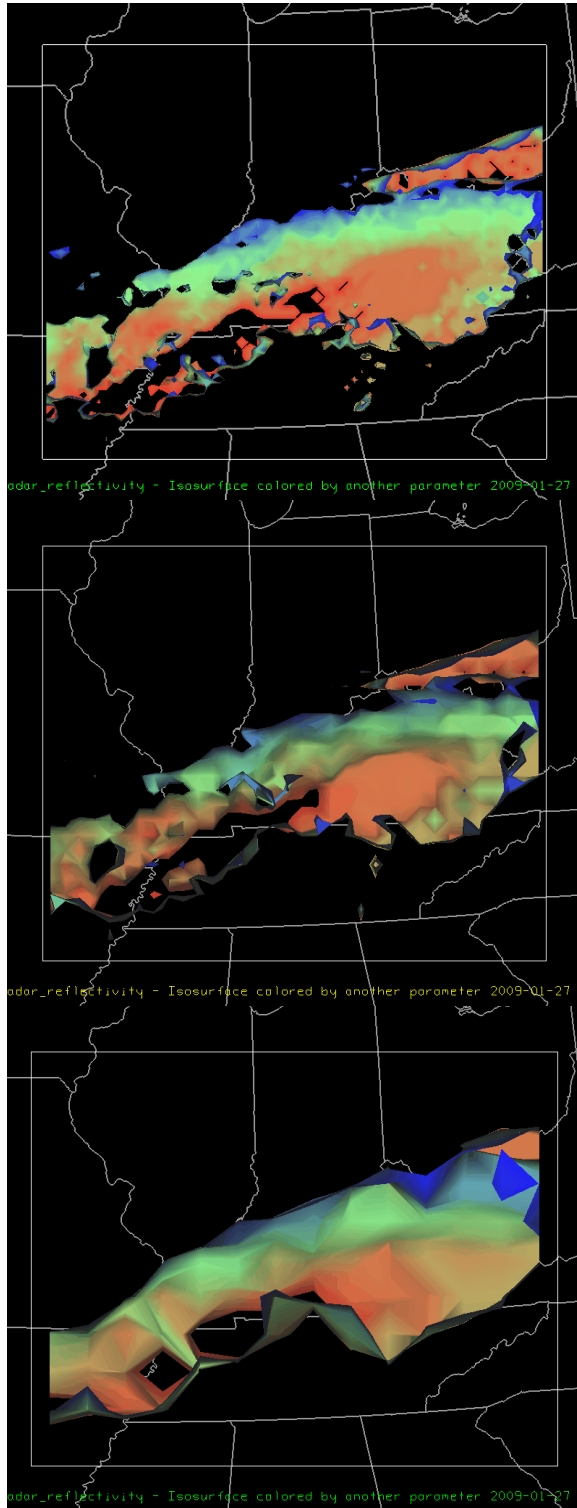


Figure 4. Height of the 25dbz surface, for MRR observations taken every (a) 13.3km, (b) 26.7km, and (c) 66.7km. Blue is 0 meters above ground level, red it 2000m above ground level.

4. CONCLUSIONS

As with any atmospheric feature, the density of observations must match the length scale of the feature. Given that the north-south extent of this transition zone is approximately 150km. As such the north-south density of an MRR network must be at least 75km. We attempted a network with 133.3km resolution (figure 5) and could not effectively observe the 25dbz surface.

FIGURE 5

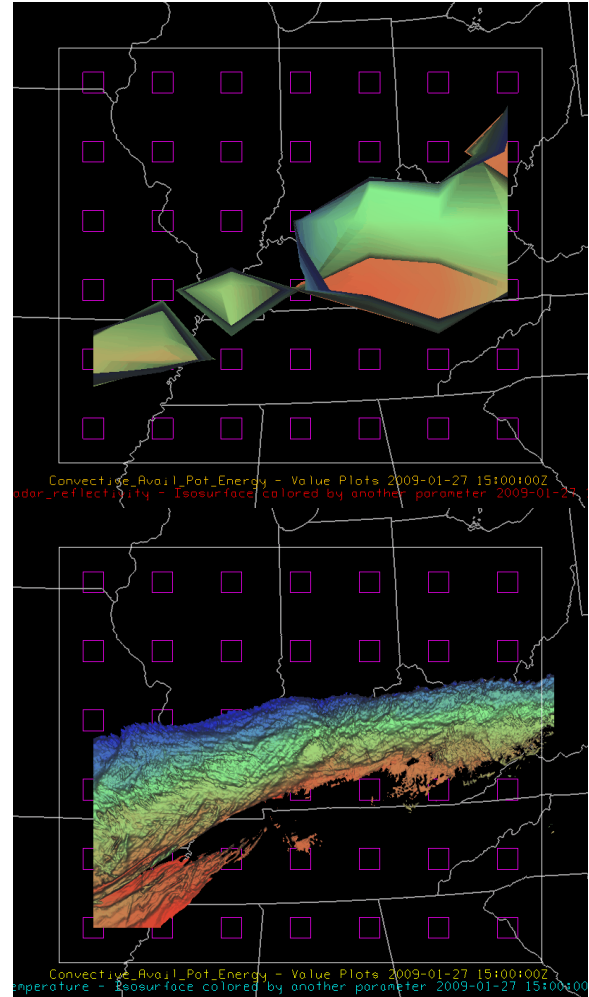


Figure 5. Height of the 25dbz surface, for MRR observations taken every 133.3km (a) and height of the 0C isosurface, data every 1.33km. Blue is 0 meters above ground level, red it 2000m above ground level. Boxes indicate observing sites.

Given that a network should have 4 or so observations across the transition zone, we recommend an MRR deployment at roughly the county scale. In addition, the observing sites should be in a climatologically likely transition zone. One such location is western North

Carolina, where there are 1-3 mixed precipitation events annually (Robinson, 2005). The area of our case study, the Ohio Valley, also is in a climatologically favored region for mixed precipitation events (Spoden, 2010, personal communication).

MRR data could provide valuable data to forecasters, overcoming a 'gap' in the observing network. The NWS WFO Raleigh has found the information useful because it provides vertical profiles that they would not otherwise have. The data is a good indicator of whether or not precipitation is hitting the ground, what type of precipitation it is, and how the depth of dry layer is changing over time. The MRR complements the present observing system.

5. ACKNOWLEDGEMENTS

We thank Unidata, the developers of the Integrated Data Viewer (IDV), which was used to generate the isosurfaces used in this study. We also thank the science operation officers (SOOs) from the National Weather Service forecast offices in Paducah, KY – Pat Spoden – and in Louisville, KY – Ted Funk – for their feedback on our study.

6. REFERENCES

Collins, W.D. et al., 2004: Description of the NCAR Community Atmosphere Model (CAM3.0), NCAR Technical Note, NCAR/TN-464+STR, 226 pp.

Ek, M. B., K. B. Mitchell, Y. Lin, B. Rogers, P. Grunmann, V. Koren, G. Gayno, and J. D. Tarpley, 2003: Implementation of Noah land surface model advances in the National Centers for Environmental Prediction operational mesoscale Eta model. *J. Geophys. Res.*, **108(D22)**, 8851.

Grumm, R. H. and J. LaCorte, 2009: The Ohio Valley Ice Storm of 27-28 January 2009. Available online at: <http://nws.met.psu.edu/severe/2009/28Jan2009.pdf>

Lang, S., W.-K. Tao, R. Cifelli, W. Olson, J. Halverson, S. Rutledge, and J. Simpson, 2007: Improving simulations of convective system from TRMM LBA: Easterly and Westerly regimes. *J. Atmos. Sci.*, **64**, 1141-1164.

Robinson, P., 2005: North Carolina Weather and Climate. University of North Carolina Press. 256pp.

Spaeth, D., G. Meffert, R. R. Smith, and P.J. Spoden, Christine Wielgos, 2009: The Lower Ohio Valley Ice Storm Of January 2009. *National Weather Association 35th Annual Meeting*, Norfolk, VA. Available online at: <http://www.nwas.org/meetings/nwa2009/presentations/NWA2009-P3.10.zip>

Sukoriansky, S., B. Galperin and I. Staroselsky, 2005: A quasi-normal scale elimination model of turbulent flows with stable stratification. *Physics of Fluids*, **17**, 085107–1–28.

Tao, W.-K., J. Simpson, D. Baker, S. Braun, M.-D. Chou, B. Ferrier, D. Johnson, A. Khain, S. Lang, B. Lynn, C.-L. Shie, D. Starr, C.-H. Sui, Y. Wang and P. Wetzell, 2003: Microphysics, radiation and surface processes in the Goddard Cumulus Ensemble (GCE) model, *A Special Issue on Non-hydrostatic Mesoscale Modeling, Meteorology and Atmospheric Physics*, **82**, 97-137.